TECHNICAL NOTE RL-252

Mi

TECHNICAL NOTE RL-252

CRATER EFFECTS ON FULL MOON DIRECTIONALITY OF LUNAR THERMAL RADIATION

by J. P. Doty

December 1967

RESEARCH LABORATORIES

BROWN ENGINEERING

A TELEDYNE COMPANY

Research Park • Huntsville, Alabama 35807

TECHNICAL NOTE R-252

CRATER EFFECTS ON FULL MOON DIRECTIONALITY OF LUNAR THERMAL RADIATION

December 1967

Prepared by

RESEARCH LABORATORIES
ADVANCED SYSTEMS AND TECHNOLOGIES GROUP
BROWN ENGINEERING, A TELEDYNE COMPANY
HUNTSVILLE, ALABAMA

By

Dr. J. P. Doty

ABSTRACT

A geometrical model of the lunar surface has been used to explain the directionality of the lunar thermal radiation from the full moon. From the model and measured data, an estimate of the crater density in certain locales has been calculated. The model assumes a lunar surface with hemispherical craters. A perturbation on the radiation intensity, caused by these craters, is added to Lambert's radiation cosine law. The resulting equation agrees very well with experimental data. With the resulting equation and a general crater distribution of $N = N_0 r^{-3}$, the local crater density is calculated.

Approved:

J. E. White, Jr.

J. E. White, Jr.
Assistant for Program Management
Advanced Systems and Technologies

Approved:

R. C. Watson, Jr.

R. C. Watson, Jr.
Vice President
Advanced Systems and Technologies

TABLE OF CONTENTS

	Page
INTRODUCTION	1
LAMBERT'S RADIATION LAW.	2
EFFECT OF CRATERS	6
LOCAL CRATER DENSITIES	21
REMARKS AND CONCLUSIONS	29
REFERENCES	30
BIBLIOGRAPHY	31

LIST OF ILLUSTRATIONS

Figure	Title	Page
1	Radiation from an Elemental Lambert Surface . . .	3
2	Area Vector $\Delta\vec{A}$ and Observational Vector $\vec{R}$	4
3	Measured Full Moon Radiation Data by Pettit and Nicholson, Compared to Radiation from Lambert Surface	7
4	Imaginary Plane Normal to the Observational Vector	8
5	Theoretical Intensity Distributions for K Values of 0.00, 0.50, and 1.00	17
6	Comparison of Pettit and Nicholson Full Moon Data and Present Predictions	18
7	Full Moon Data (Ingrao et al.) Compared with Present Predictions	19
8	Thermal Coordinate Grid for Phase Angle -2°16'. .	22
9	Local N_0 Values Along the 30° Thermal Latitude . .	24
10	Local N_0 Values Along the 40° Thermal Latitude . .	25
11	Local N_0 Values Along the 50° Thermal Latitude . .	26
12	Local N_0 Values Along the 60° Thermal Latitude . .	27
13	Cumulative Local Lunar Crater Distribution for $N_0 = 0.02$ [Plot of $N' = (1/2) N_0 r^{-2}$]	28

LIST OF SYMBOLS

A	Constant used by Miller in the cumulative crater density equation
ΔA	Elemental area which is radiating
$\Delta \vec{A}$	Area vector of the incremental area ΔA
A_R	Resolution area (on a perpendicular plane) of the measuring instrument
$(A_R)_{IP}$	Resolution area on the imaginary plane
$(A_R)_{LS}$	Resolution area on the lunar surface
a	Lower limit of crater radius to be considered
B	Exponent of the diameter for the cumulative crater density (used by Miller)
$B(\theta)$	Luminance of a surface
B_0	Luminance of a Lambert surface
b	Upper limit of crater radius to be considered
D	Diameter of the crater (used by Miller)
$I(\theta)$	Radiated intensity from a surface
I_0	Radiated intensity normal to the surface
$I_{c.f.}$	Intensity of radiation from a circular flat area
I_{crater}	Intensity of radiation from just one hemispherical crater
K	Magnitude of perturbation term (K' - general; K_1 - associated with the imaginary plane; K_2 - associated with the lunar surface)
m	General exponent of radius for crater density
N	Number of craters of radius r per unit area

LIST OF SYMBOLS - Concluded

N'	Number of craters (whose radius is r or larger) per unit area
N_0	Constant of proportionality for crater density
n	Number of craters in the resolution area
$\vec{R}$	Observational vector or vector in the direction of the line of radiation measurement
r	Radius of a crater or circular area
δ	Intensity perturbation term
θ	Angle between the line of measured radiation and the surface perpendicular

INTRODUCTION

The directionality of the measured full moon lunar thermal radiation differs from that of a perfectly diffuse body which radiates according to Lambert's cosine law. The intensity of thermal radiation (8-12 micron region) from the full moon is greater at intermediate angles than is predicted for a slowly rotating, diffuse sphere. Pettit and Nicholson (Ref. 1) suggest that the surface roughness is the cause of the deviation in directionality. They and other authors have used different models in an attempt to reproduce the measured data.

To explain this particular directionality, a mathematical model of the lunar surface is used in the following development. The model consists of the lunar surface pockmarked with various size hemispherical craters. The directionality of the reradiated infrared from such a model is shown to closely resemble that of the full moon measurements.

Other authors have considered similar theoretical models; among these are Markov (Ref. 2) and Schoenberg (Ref. 3). From the developed equations in this investigation, the local crater density is calculated where thermal radiation data have been measured. The crater distribution in the Ranger series of high resolution photographs is used as a check on the model used here.

The model assumes all craters are hemispherical in shape, with their axes of rotation perpendicular to the lunar surface. These craters are assumed to cover a percentage of the lunar surface, with all sizes contributing to any particular measurement. The surface in very small areas is assumed perfectly diffuse. This means that crater walls and surfaces between craters are perfectly diffuse and that each elemental small area radiates according to Lambert's cosine law. It is further assumed that the temperature on the sunlit portion of the crater wall is uniform and equal to the temperature of the surrounding sunlit area.

LAMBERT'S RADIATION LAW

The radiation intensity from a Lambert surface (i.e., perfectly diffuse) is expressed as

$$I(\theta) = I_0 \cos \theta \tag{1}$$

where I_0 is the intensity that is radiated perpendicular to the surface and θ is the angle between the viewing direction and the surface normal. The luminance* is defined by

$$B(\theta) = \frac{I}{\Delta A \cos \theta} \tag{2}$$

for a flat surface. Note, $B(\theta)$ is a constant for a Lambert surface. Radiation from a surface ΔA is illustrated in Figure 1.

For complex surfaces and surfaces that are not flat, Lambert's radiation cosine law becomes awkward in its usual form. This radiation law can be expressed in a more flexible form:

$$I(\theta) = I_0 \left(\frac{\Delta\vec{A}}{|\Delta A|} \cdot \frac{\vec{R}}{|R|} \right) \tag{3}$$

where $\Delta\vec{A}$ is the area vector whose direction is perpendicular to the surface and whose magnitude is equal to the area of the surface. The observational vector $\vec{R}$ is directed toward the observer. The quantities $\Delta\vec{A}/|\Delta A|$ and $\vec{R}/|R|$ are unit vectors in the specified directions. Figure 2 shows these vectors located on a flat elemental surface. The luminance can be written in a dot product form of

$$B(\theta) = \frac{I_0 \left(\frac{\Delta\vec{A}}{|\Delta A|} \cdot \frac{\vec{R}}{|R|} \right)}{\left(\Delta\vec{A} \cdot \frac{\vec{R}}{|R|} \right)} \quad . \tag{4}$$

*The term luminance is often replaced by the word brightness. Luminance is an objective word whereas brightness is subjective and is a function of the observer's spectral and intensity response.

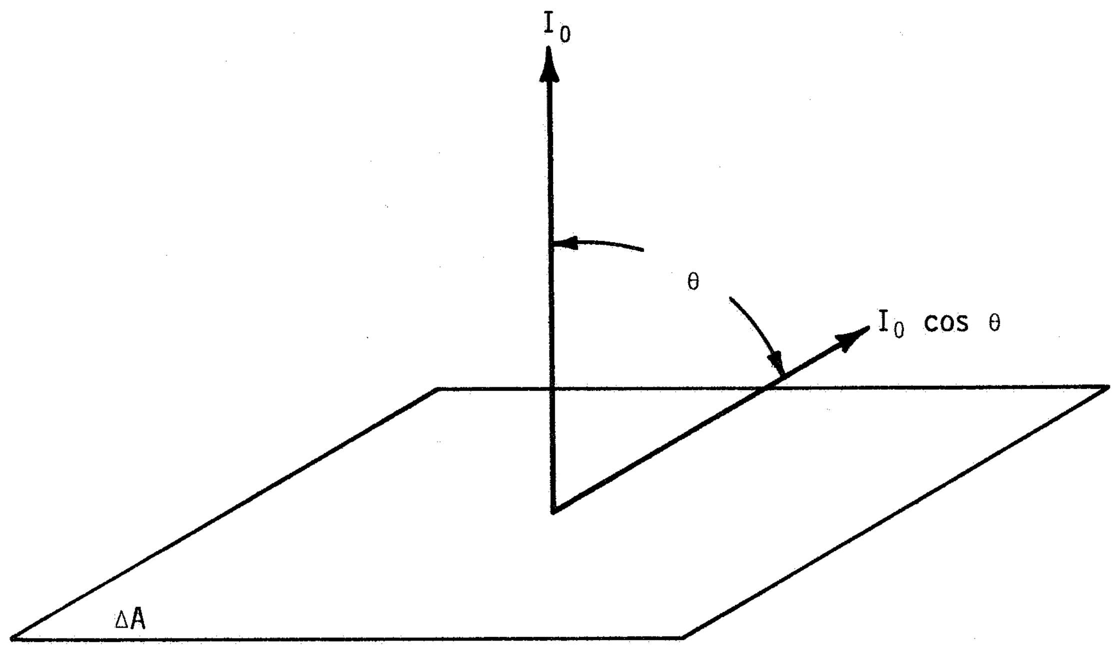

FIGURE 1. RADIATION FROM AN ELEMENTAL LAMBERT SURFACE

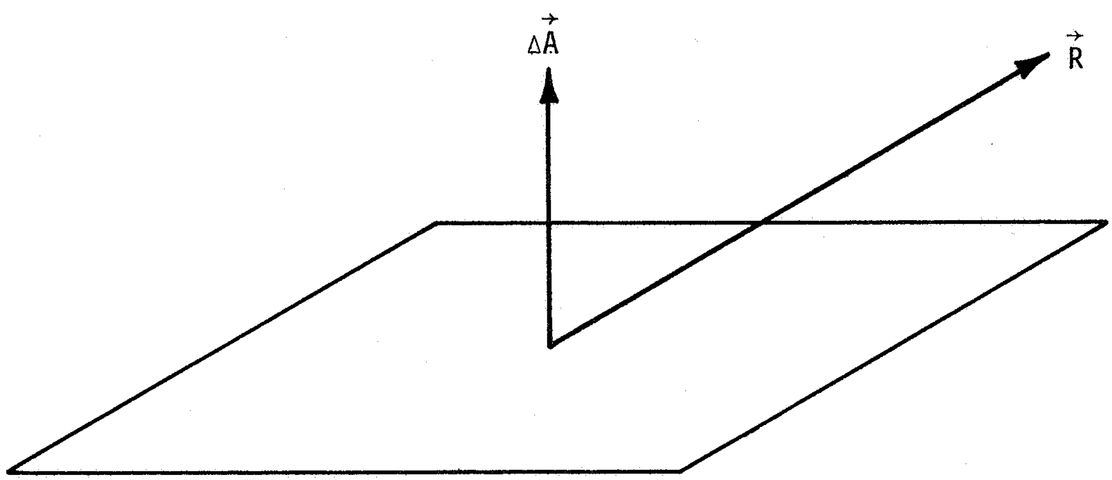

FIGURE 2. AREA VECTOR $\Delta\vec{A}$ AND OBSERVATIONAL VECTOR $\vec{R}$

The parameter B_0 is defined from Equation 4 when the angles from the dot products are equal

$$B_0 = \frac{I_0}{|\Delta A|} \quad . \tag{5}$$

The radiated intensity from a Lambert surface, Equation 3, can be related to the radiating area.

$$I(\theta) = B_0 \left(\Delta\vec{A} \cdot \frac{\vec{R}}{|R|} \right). \tag{6}$$

The intensity of radiation from a surface can be expressed in a number of ways as demonstrated by Equation 1, Equation 3, and Equation 6. One should keep in mind that Lambert's law is an empirical description only and is not a function of the radiating area. Equation 6 displays the intensity as a function of the area but it must be realized that B_0 is also a function of ΔA in such a way that $I(\theta)$ is a function of the angle θ only. The luminance is a function of the radiating area (see Equation 2) and, specifically, is inversely proportional to the projected area.

EFFECT OF CRATERS

The radiation from an area containing craters will have a directionality different from that of a Lambert surface. The effect of such a crater area can be considered as a perturbation to the radiation, so that the intensity can be written:

$$I(r, \theta) = I_0 \cos \theta + \delta (r, \theta) \tag{7}$$

or

$$I(r, \theta) = I_0 \left(\frac{\Delta \vec{A}}{|\Delta A|} \cdot \frac{\vec{R}}{|R|} \right) + \delta(r, \theta) . \tag{8}$$

Here, δ is the perturbation due to the craters and is a function of the crater radius (r) and the angle θ. In the development of the perturbation term, one considers the crater geometry, crater size, the distribution of the crater size, and the resolution area of the observing instrument. Figure 3 illustrates the deviation of the measured thermal data from the radiation of a Lambert surface (the dashed line). The perturbation term is postulated to account for the difference between the measured intensity and that radiated by a perfectly diffuse surface. The deviation, as seen in Figure 3, is due to the actual lunar craters; however, in the mathematical model, hemispherical craters are assumed to illustrate the properties of this lunar surface model.

To develop an expression for lunar intensity, the lunar surface is projected onto an imaginary flat plane which is perpendicular to the line of sight or observational vector. A circular area on the lunar surface and its projection onto the flat imaginary plane are illustrated in Figure 4. The projected flat circular area appears elliptical on the imaginary plane. Therefore, the radiating area from the plane is

$$|\Delta A|_{obs} = \pi r^2 \cos \theta \tag{9}$$

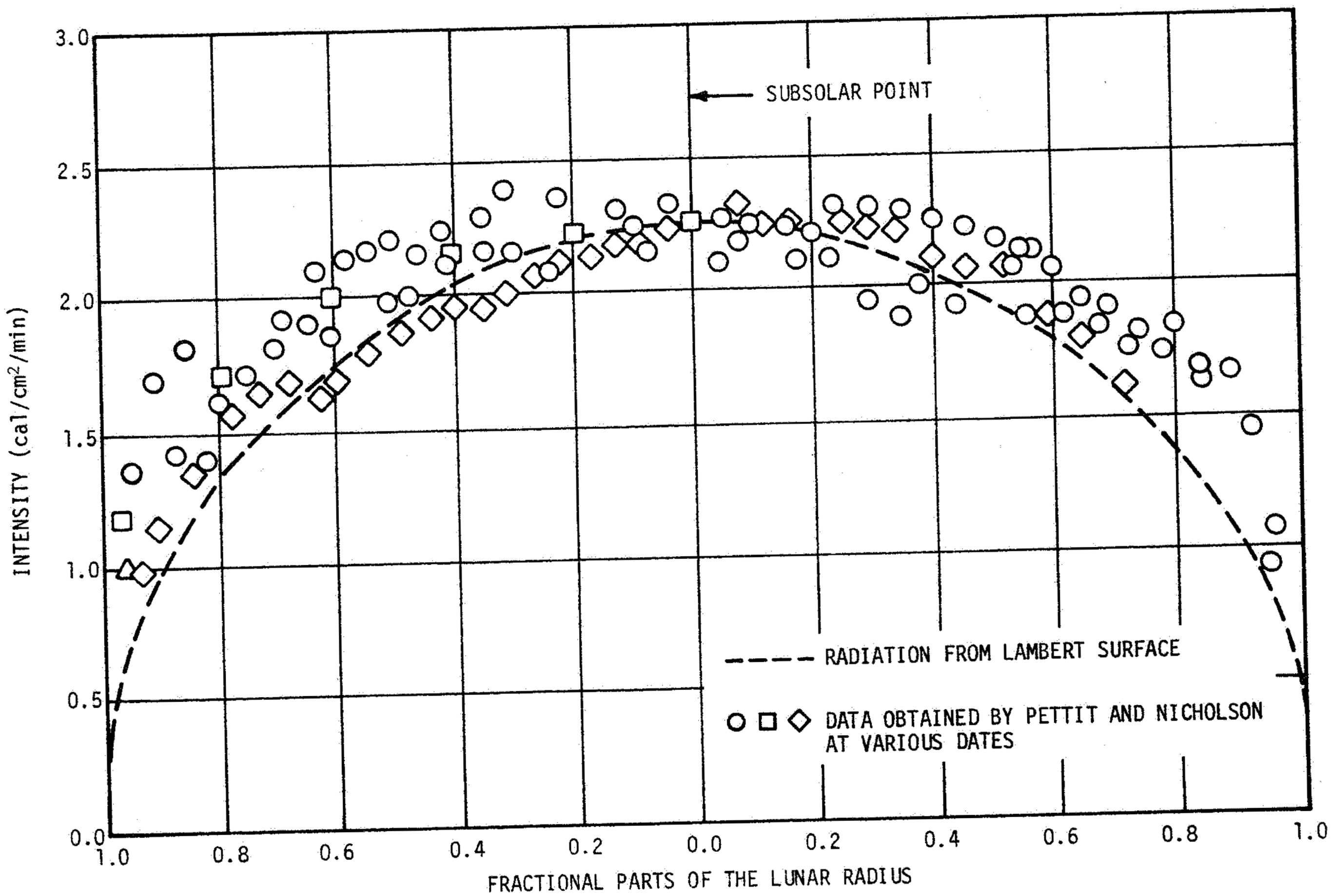

Figure 3. Measured Full Moon Radiation Data by Pettit and Nicholson, Compared to Radiation from Lambert Surface

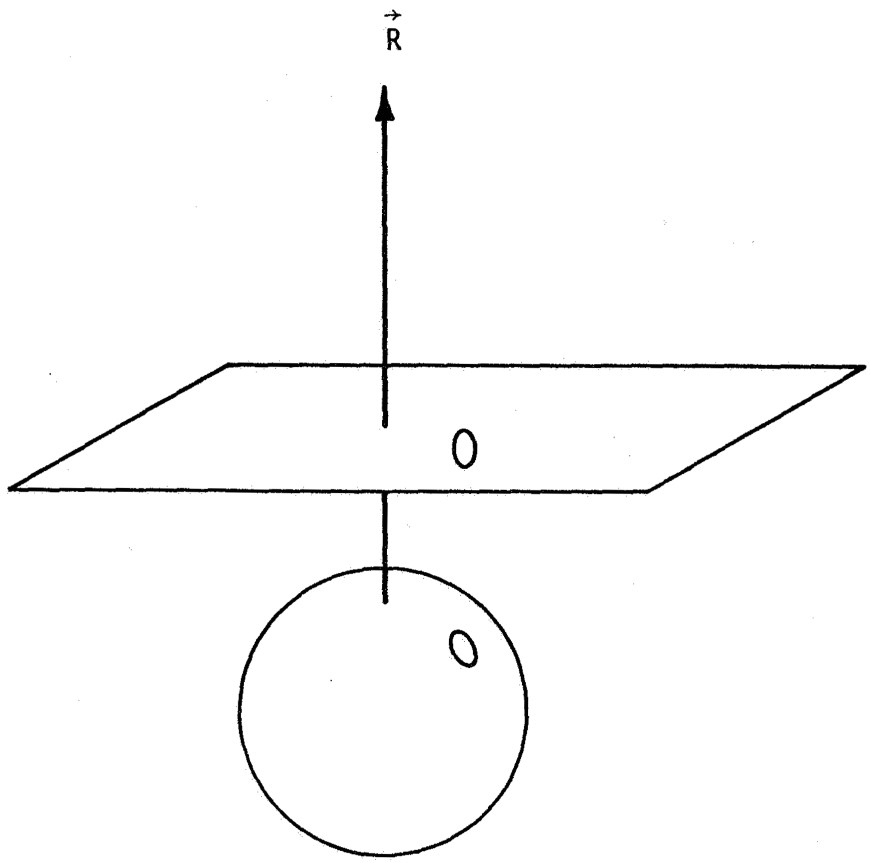

FIGURE 4. IMAGINARY PLANE NORMAL TO THE OBSERVATIONAL VECTOR

which is the same as that projected by a hemispherical crater. This is to say that Equation 9 holds true for either a projected flat circular area on the lunar surface or a projected hemispherical crater opening on the lunar surface.

The intensity, radiating through the imaginary plane from a point on the lunar surface, can be written as:

$$I(\theta) = I_0 \cos \theta \quad . \tag{10}$$

If this point is expanded to a finite area, Equation 10 is still valid. Equation 10 is associated with the lunar surface. The intensity can be written as a function of the luminance utilizing Equation 6. The area of interest is a flat circular area and is projected onto the imaginary plane. The angle θ has been described, and the magnitude of the area on the imaginary plane is given by Equation 9. The intensity from this elliptical area on the imaginary plane is

$$I_{c.f.} = B_0 (\pi r^2 \cos \theta) \cos \theta$$

$$I_{c.f.} = B_0 \pi r^2 \cos^2 \theta \quad . \tag{11}$$

The intensity given by Equation 11 refers to the area on the imaginary plane. To relate the intensity to the lunar surface, a substitution must be made. Substituting for B_0 and for $|\Delta A|_{obs}$ of Equation 5 into Equation 11, the intensity for the circular flat area on the lunar surface is

$$I_{c.f.} = I_0 \cos \theta \tag{12}$$

which is identical to Equation 10. Equation 12 pertains to the lunar surface and is not a function of the circular area.

The thermal intensity radiating from a hemispherical crater can be written in either form presented above. The vector dot product in Equation 6 can be evaluated directly as the projection of the crater area on the imaginary plane. The intensity radiating from the imaginary plane is

$$I_{crater} = B_0 \pi r^2 \cos \theta \quad . \tag{13}$$

Substituting for B_0 and $|\Delta A|$ on the imaginary plane, Equation 13 becomes

$$I_{crater} = I_0 \tag{14}$$

which is the intensity from a hemispherical crater on the lunar surface. The thermal radiation from both a flat circular area and a hemispherical crater has now been obtained for two different reference systems.

A note should be made at this point concerning the radiation from a Lambert sphere. The equation $I(\theta) = I_0 \cos \theta$ describes the radiation from the entire visible surface of the sphere. The inclusion of craters on the surface implies that the craters replace some of the area which has already been considered in Lambert's radiation law. To form the intensity from a cratered lunar surface, the intensity due to the crater is added to the intensity due to a perfectly diffuse Lambert sphere; and the intensity due to the flat circular area, which the crater displaced, is subtracted from this sum. The perturbation term will have a factor which is the difference between the intensity from one crater and the intensity from a flat circular area. In the development so far, only one crater has been considered; but in a realistic model, a large number of craters must be included. Each hemispherical crater radiates with the same directionality. Only the magnitude of the intensity will change with an increase in craters. A simple increase occurs for craters of increasing radius. The perturbation term is proportional to the directionality factor and can be written as

$$\delta(r, \theta) = K'(I_{crater} - I_{c.f.}) \tag{15}$$

where K' is the proportionality constant. The substitutions for I_{crater} and $I_{c.f.}$ can be made from either set of equations but both must have the same reference surface. The expressions for $I_{c.f.}$ and I_{crater} from

Equations 11 and 13, which are associated with the imaginary plane, are substituted into Equation 15.

$$\delta(r,\theta) = K'(B_0 \pi r^2 \cos\theta - B_0 \pi r^2 \cos^2\theta) \quad . \tag{16}$$

There are a number of constants (if only one crater is considered) in Equation 16; these are K', B_0, π, r. Substituting for B_0 and combining all of these constants into a new constant yields

$$\delta(r,\theta) = I_0 K_1 (\cos\theta - \cos^2\theta) \tag{17}$$

where the parenthetical factor gives the directionality and $I_0 K_1$ the magnitude of the perturbation. Equation 17 is also referenced to the imaginary plane.

To develop the equation with the lunar surface as the reference surface, the expression for $I_{c.f.}$ and I_{crater} from Equation 12 and 14 are substituted into Equation 15:

$$\delta(r,\theta) = K_2 (I_0 - I_0 \cos\theta) \tag{18}$$

or

$$\delta(r,\theta) = I_0 K_2 (1 - \cos\theta) \quad .$$

The perturbation term considers the crater geometry, crater size, distribution of crater size, and the instrumental area of resolution. To this point in the development, only the crater geometry and one crater have been considered. All other listed items must now be considered.

A note should be made concerning the reference surface; the resolution area is different for each. To define the resolution area, it is the area (on the lunar surface or imaginary plane) from which the radiation is emitted and thus measured by the sensor mechanism for each data point. The resolution area is circular for the imaginary plane. The resolution area is elliptical for the lunar surface reference and so a function of the angle θ. The resolution area for the lunar surface is

$$(A_R)_{LS} = (A_R)_{IP} (1/\cos\theta) \tag{19}$$

where $(A_R)_{LS}$ is the resolution area on the lunar surface, and $(A_R)_{IP}$ is the resolution area on the imaginary plane.

The magnitude of the perturbation term is the ratio of the area consumed by craters to the total possible area. The area each crater consumes is πr^2. If there are n craters in the resolution area, the fraction of the area consumed by craters, which have radius r, is

$$\left(\frac{\text{area consumed by craters}}{\text{total available area}}\right)_{LS} = \frac{n \pi r^2}{(A_R)_{LS}} \tag{20}$$

or

$$\left(\frac{\text{area consumed by craters}}{\text{total available area}}\right)_{IP} = \frac{n \pi r^2}{(A_R)_{IP}} \quad . \tag{21}$$

Equation 20 is associated with the lunar surface, and Equation 21 is associated with the imaginary plane. Substituting for $(A_R)_{LS}$ from Equation 19 into Equation 20 yields

$$\left(\frac{\text{area consumed by craters}}{\text{total available area}}\right)_{LS} = \frac{n \pi r^2}{(A_R)_{IP}} \cos\theta \quad . \tag{22}$$

It is convenient to use the resolution area referenced to the imaginary plane which is perpendicular to the line of sight. The resolution area $(A_R)_{IP}$, which is referenced to the imaginary plane, will be considered as the resolution area and will be denoted as A_R, or that is

$$(A_R)_{IP} = A_R \quad . \tag{23}$$

The size of the craters is now allowed to vary so that a range of radii can be considered. The incremental value for K_1 of Equation 17 (which is for the imaginary plane), is obtained from Equation 21 and is for radii between r and r + dr.

$$d\,K_1 = (n/A_R)\,\pi\,r^2\,dr \quad . \tag{24}$$

The incremented value for K_2 of Equation 18 (which is for the lunar surface), is obtained in a similar method from Equation 22:

$$d\,K_2 = (n/A_R)\,\pi\,r^2\cos\theta\,dr \quad . \tag{25}$$

From the incremental value $d\,K_1$, the value of K_1 can be determined by integrating; therefore, integrating Equation 24 with respect to the radius yields

$$K_1 = \int_a^b (n/A_R)\,\pi\,r^2\,dr \quad . \tag{26}$$

where a is the lower limit of integration on the radius and b, the upper limit. An explicit expression for (n/A_R) is needed before the integration (on the right-hand side of the above equation) can be performed. The value of K_2 can be determined in a like manner to Equation 26.

$$K_2 = \cos\theta \int_a^b (n/A_R)\,\pi\,r^2\,dr \quad . \tag{27}$$

Substituting K_1 from Equation 26 into Equation 17 yields an expression for the perturbation term that is referred to the imaginary plane:

$$\delta(r,\theta) = I_0 \left[\int_a^b (n/A_R)\,\pi\,r^2\,dr\right](\cos\theta - \cos^2\theta) \quad . \tag{28}$$

Substituting K_2 from Equation 27 into Equation 18 yields another expression for the perturbation term that is associated with the lunar surface:

$$\delta(r,\theta) = I_0 \left[\cos\theta \int_a^b (n/A_R)\,\pi\,r^2\,dr\right](1 - \cos\theta) \quad . \tag{29}$$

Rearranging both Equations 28 and 29, each can be put into the form

$$\delta(r, \theta) = I_0 \cos\theta\,(1 - \cos\theta) \int_a^b (n/A_R)\,\pi\, r^2\, dr \quad . \tag{30}$$

As seen from Equation 30, the expression can be developed through the use of either reference surface. The equations were developed in parallel to demonstrate this conclusion. From this point on, the parallel exposition will be dropped and a single avenue of approach adopted. From Equation 30, a constant K can be defined so that I_0 K is the magnitude of the perturbation term.

$$\delta(r, \theta) = I_0\, K(\cos\theta - \cos^2\theta) \tag{31}$$

$$K = \int_a^b (n/A_R)\,\pi\, r^2\, dr \quad . \tag{32}$$

The perturbation term has now considered crater geometry and the instrumental area of resolution, but not the distribution of crater size. The lunar cumulative crater size distribution has been measured by McGillen and Miller (Ref. 4). They have compiled statistical data on the size distribution of craters in the range of sizes visible on lunar maps and photographs. The data was fit by the equation

$$N' = AD^{-B} \tag{33}$$

where N' is the number of craters, having diameter greater than D, per area, and A and B are constants. (B here is not to be confused with luminance $B(\theta)$; they are completely different.) The negative derivative of Equation 33 yields the number of craters per unit area having a diameter D. A substitution of 2r is made for D and for redefining the constants

$$N = N_0\, r^{-m} \tag{34}$$

where N is the number of craters (of radius r) per unit area, and N_0 and m are constants. According to a number of investigations, the exponent B in Equation 33 has a value ranging from 1.6 to 2.12, which gives a value to m in Equation 34 of 2.6 to 3.12. An arbitrary value of 3.00 was chosen for m, so that Equation 34 becomes

$$N = N_0 \; r^{-3} \quad . \tag{35}$$

The cumulative crater density is in the same form as Equation 33, which is $N' = \frac{1}{2} N_0 \; r^{-2}$. The number of craters per unit area in the formulation of K was in the form of (n/A_R), so that (n/A_R) and N can be equated:

$$(n/A_R) = N \quad . \tag{36}$$

Substituting Equation 36 into Equation 35 and substituting the resulting equation into Equation 32 yields

$$K = \int_a^b N_0 \; \pi \; r^{-1} \; dr \quad . \tag{37}$$

Performing the integration yields an algebraic expression for the value of K:

$$K = N_0 \; \pi \; \ell n \; (a/b) \quad . \tag{38}$$

In developing Equation 38, crater size distribution, area of resolution, and total number of craters within a given measurement have been considered.

The perturbation term can be stated in full

$$\delta(r, \theta) = I_0 \; N_0 \; \pi[\ell n \; (a/b)] \; (\cos \theta - \cos^2 \theta) \tag{39}$$

or can be left in the form

$$\delta(r, \theta) = I_0 \; K(\cos \theta - \cos^2 \theta) \quad . \tag{40}$$

To recapitulate its development, the perturbation term considered the crater geometry, crater size, distribution of crater size, and the instrumental area of resolution. The I_0 K factor is the magnitude, and the parenthetical factor in Equation 40 is the directionality of the perturbation.

The radiation from a full moon that contains craters can be obtained by substituting Equation 39 into Equation 7:

$$I(r, \theta) = I_0 \cos \theta + I_0 N_0 \pi [\ell n (a/b)] (\cos \theta - \cos^2 \theta) \tag{41}$$

or

$$I(r, \theta) = I_0 \cos \theta \{1 + N_0 \pi [\ell n (a/b)] (1 - \cos \theta)\} . \tag{42}$$

Substituting Equation 38 into Equation 42 yields

$$I(r, \theta) = I_0 \cos \theta [1 + K(1 - \cos \theta)] \tag{43}$$

where $K = N_0 \pi \ell n (a/b)$. Either form of Equation 42 or Equation 43 describes the radiation from the full moon. Equation 43 considers the magnitude of the perturbation as determined by a constant (which is to be used to fit measured data); and Equation 42 considers the crater size distribution et al. A plot of Equation 43 for three values of K (0.00, 0.50, and 1.00) is shown in Figure 5. Equation 42 is to be used to calculate a value of intensity which predicts a measured value before the measurement. Therefore, each of these equations is useful for its particular purpose.

Utilizing Equation 43, the Pettit and Nicholson (Ref. 1) full moon data are matched with a value of $K = 0.46$. Figure 6 shows Equation 43 fitted to the Pettit and Nicholson data. The dotted line is the radiation from a Lambert surface. The full moon data of Ingrao et al (Ref. 5) was also fitted by the curve from Equation 43. The resulting K value was $K = 0.47$. The full moon data published by Ingrao et al is shown in Figure 7 where the solid line in Equation 43 with $K = 0.47$ and the dotted line is the same as in Figure 5.

These values of K were obtained by using a "least-squares" method of fitting the curve to the set of points. Fitting an entire set of full moon

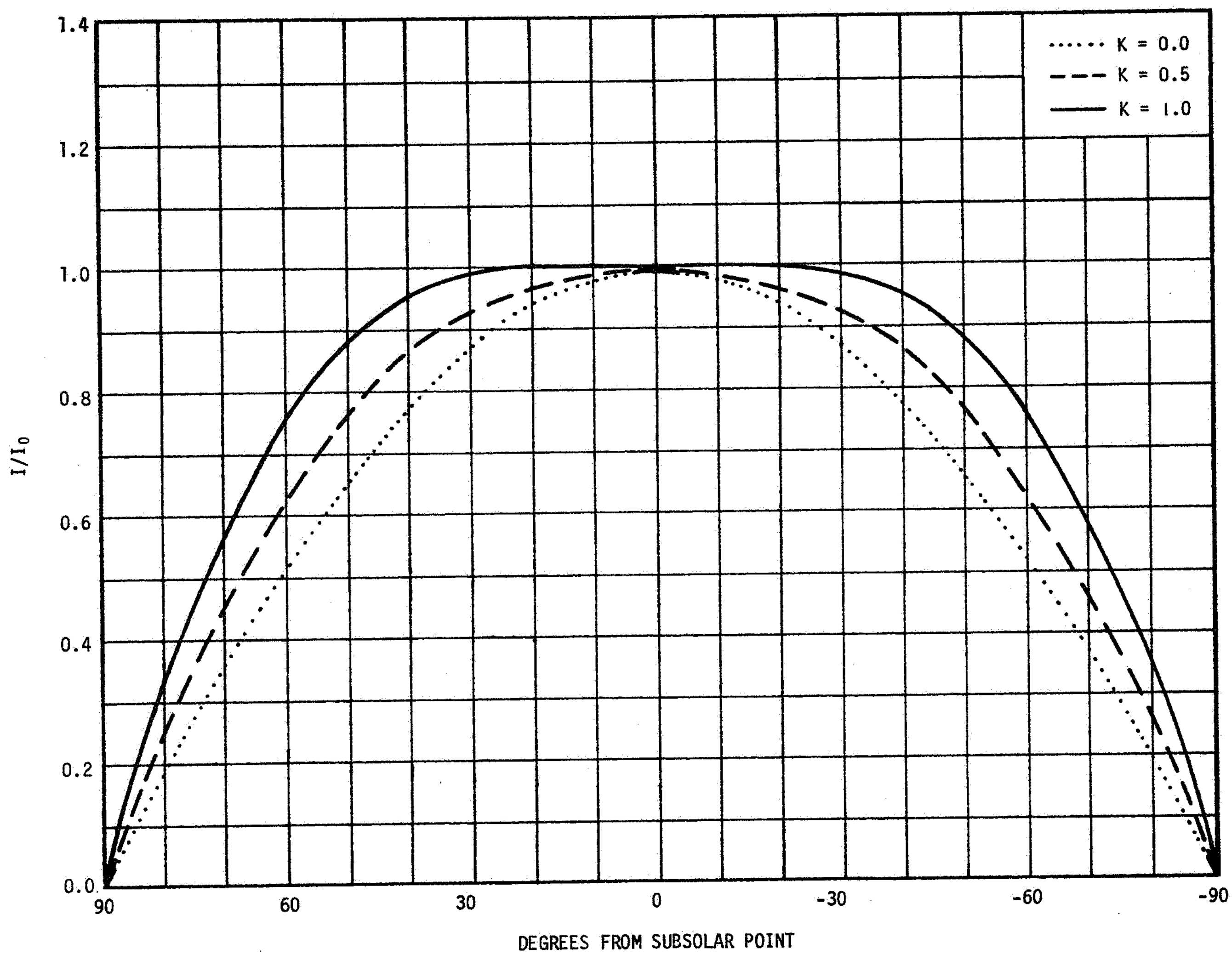

FIGURE 5. THEORETICAL INTENSITY DISTRIBUTIONS FOR K VALUES OF 0.00, 0.50, AND 1.00

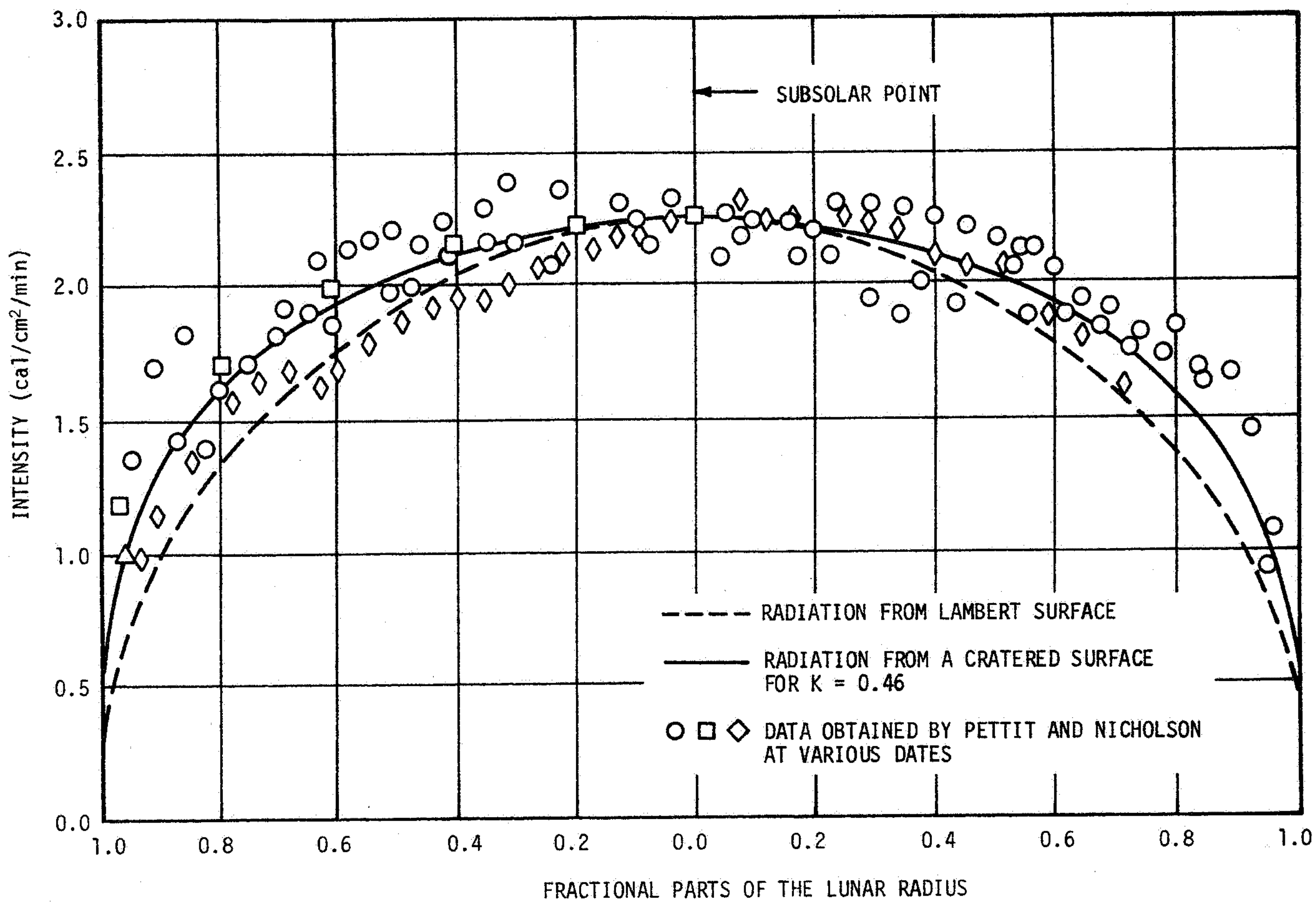

FIGURE 6. COMPARISON OF PETTIT AND NICHOLSON FULL MOON DATA AND PRESENT PREDICTIONS

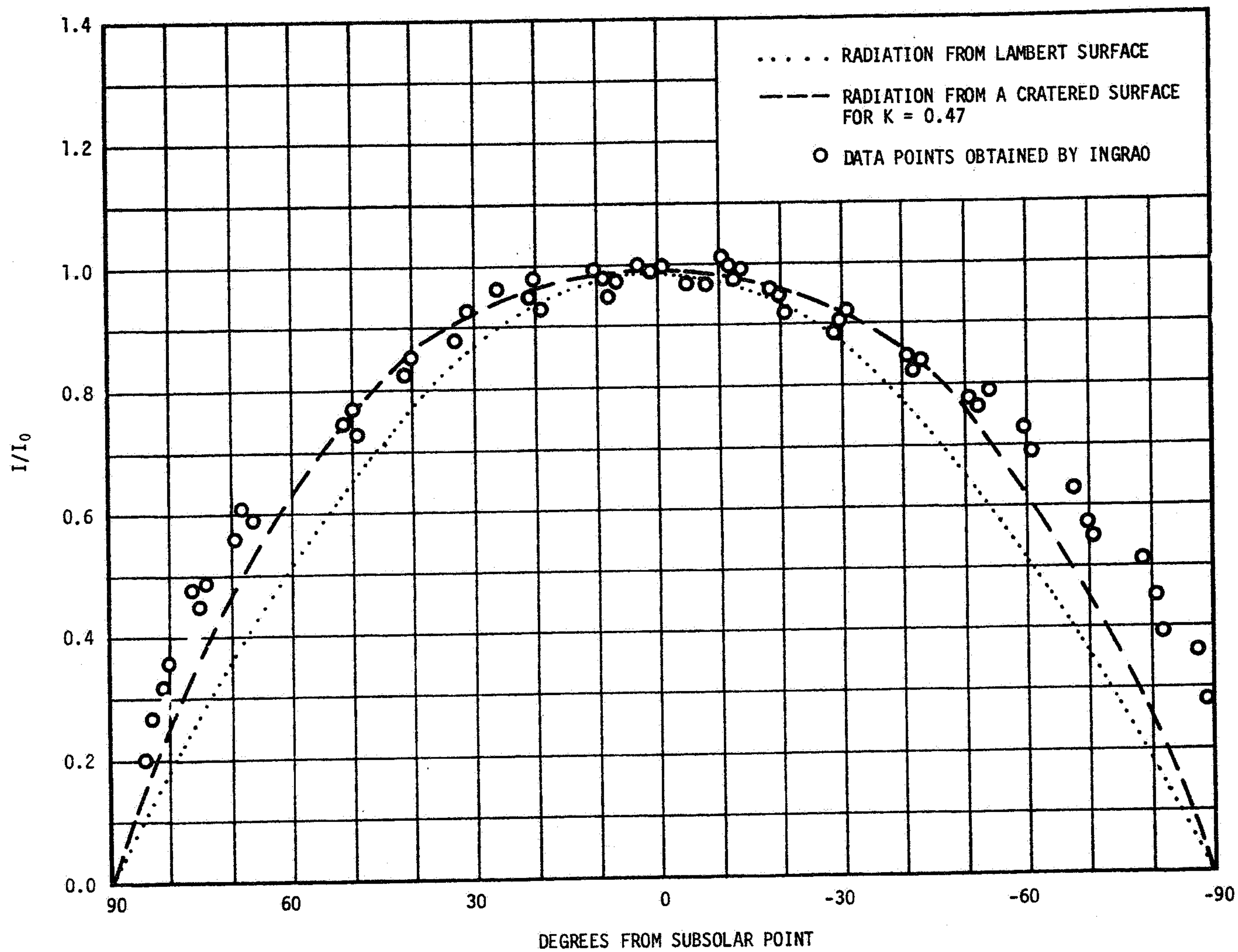

FIGURE 7. FULL MOON DATA (INGRAO ET AL.) COMPARED WITH PRESENT PREDICTIONS

data yields an equation that approximately describes the entire surface of the Moon.

The value of K can be obtained from Equation 43 for individual measurements, but Equation 42 may be used instead. If the measurement is located precisely on the lunar surface and the limits on the crater radii are known, Equation 42 is solved for the constant N_0. Another use of Equation 42 is for predicting $I(r, \theta)$ before a measurement is made. For this purpose, the limits on the crater radii are selected from previously obtained data (e. g., photographs); the constant N_0, which is a function of the crater density, is obtained from a tabulation of N_0 or an average value; and the position on the surface of the full moon is located. With this information, Equation 42 can be solved for $I(r, \theta)$, which is the predicted intensity, and is calculated without an intensity measurement.

LOCAL CRATER DENSITIES

The crater density N can be calculated for each measured data point. The value of K calculated from Equation 43 for each measured point can be used in conjunction with Equation 38 to determine the constant N_0 for a locale on the lunar surface. To utilize Equation 38, the upper limit of the crater radius and the corresponding lower limit must be measured or calculated. An upper limit, b, is selected from telescopic photographs of the same area as the thermal measurements and is numerically equal to the radius of the largest crater in this resolution area. If there are no measurable craters within the photographed area, an arbitrarily selected radius of five kilometers is taken for the upper limit. The lower limit of the crater radius, a, is taken as 0.01 kilometers. This particular lower limit was selected because all craters smaller than this would add only 0.1 percent to the numerical value of the perturbation term. The measuring apparatus has a sensitivity or accuracy of greater than 0.1 percent. Craters of radius one meter and smaller only tend to produce a diffuse surface when observed with an instrumental resolution of ten kilometers or more. Thus, with the chosen limits and a calculated value of K, all for one locale on the lunar surface, the constant N_0 can now be calculated from Equation 38. The constant N_0 is directly related (through Equation 35) to the crater density at that particular locale on the lunar surface. Therefore, with N_0 known, the local crater density can be calculated.

The lunar thermal radiation data obtained by Shorthill and Saari and published by Montgomery et al (Ref. 6) is well documented as to the exact lunar location. These data points are at the intersections of the thermal latitudes and thermal longitudes. This coordinate system is shown in Figure 8 where the subsolar point is the origin. For the numerical calculations, a consistent set of units must be used; these are

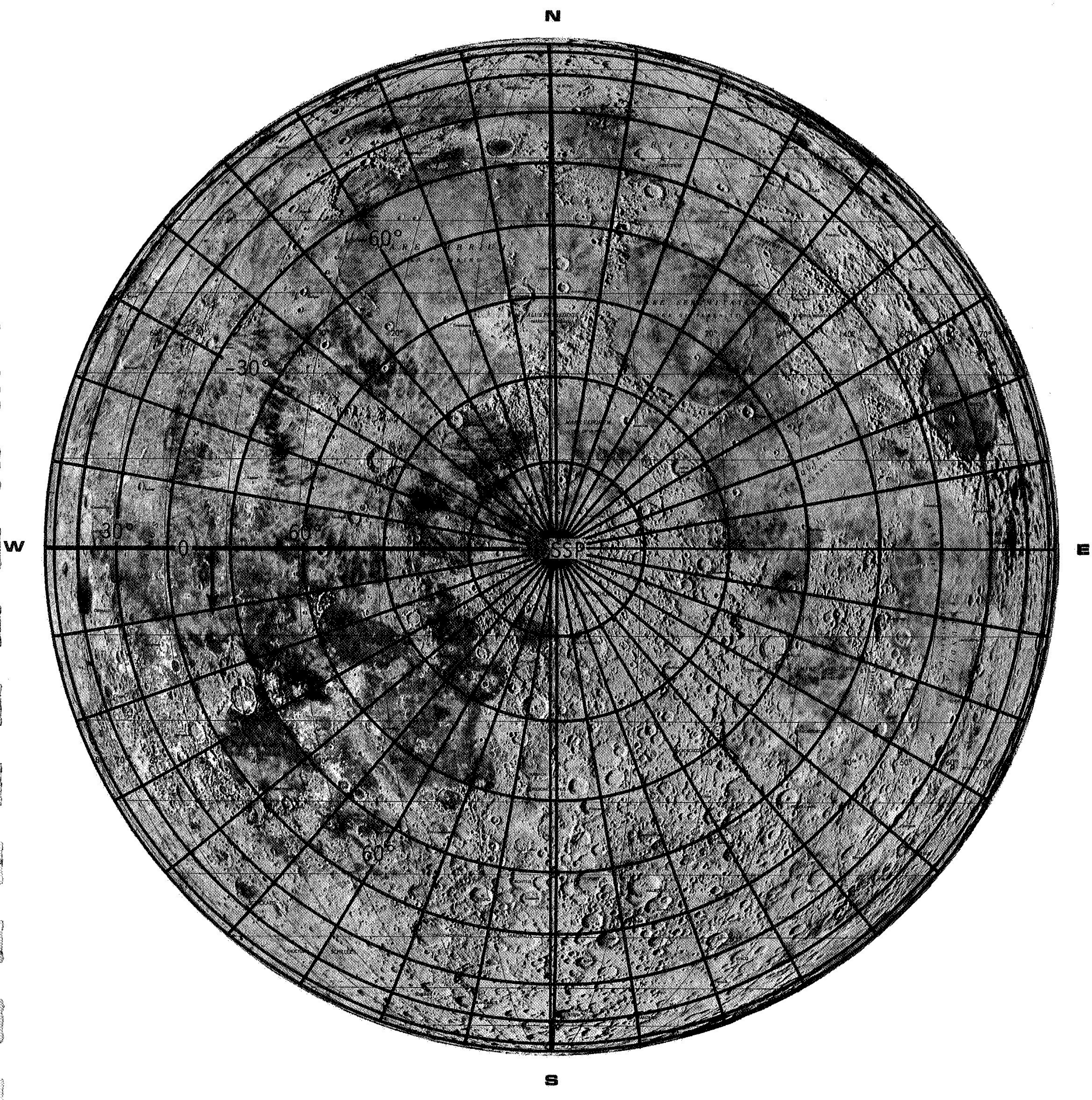

FIGURE 8. THERMAL COORDINATE GRID FOR PHASE ANGLE (-2°16')

unit radius	-	one kilometer
unit area	-	one square kilometer
N	-	number of craters (having radius r in kilometers) per square kilometer.

Calculated local values for the constant N_0 along the thermal longitude intersections with the 30-degree thermal latitude are shown in Figure 9. Values of N_0 for the 40-, 50-, and 60-degree thermal latitudes are shown in Figures 10, 11, and 12, respectively. Each of these values for N_0 can be used to calculate the local cumulative crater density (the number of craters of radius r or greater in an area of one square kilometer) at each of the locales. Figure 13 is a graph of the equation $N' = \frac{1}{2} N_0 \; r^{-2}$ where $N_0 = 0.02$. The cumulative crater density for any locale can be obtained by reading a value from Figure 13, by multiplying this value by the N_0 of that locale (found from Figure 9, 10, 11, or 12), and by dividing the product by 0.02.

To examine a comparison between a measured crater density and that calculated by the method previously developed, the Ranger VII photographs are utilized. Miller (Ref. 7), performed a size frequency study of craters appearing in the Ranger VII photographs. Miller fitted a straight line of the form $\log N = \log A + B \log D$ to the data obtained from the photographs. Two sets of diameter ranges were used, one greater than 1.75 kilometers, the other less than 1.75 kilometers. The comparison with the lower range is more meaningful since the extrapolation of interest is toward the smaller size. The landing site of the Ranger VII is not too distant from the coordinates of 20 degrees thermal longitude and 60 degrees thermal latitude. Selecting the values of N_0 from this locale and comparing, after adjustment has been made for difference in units, with the Miller measurement, the calculated density is four times greater than the measured density.

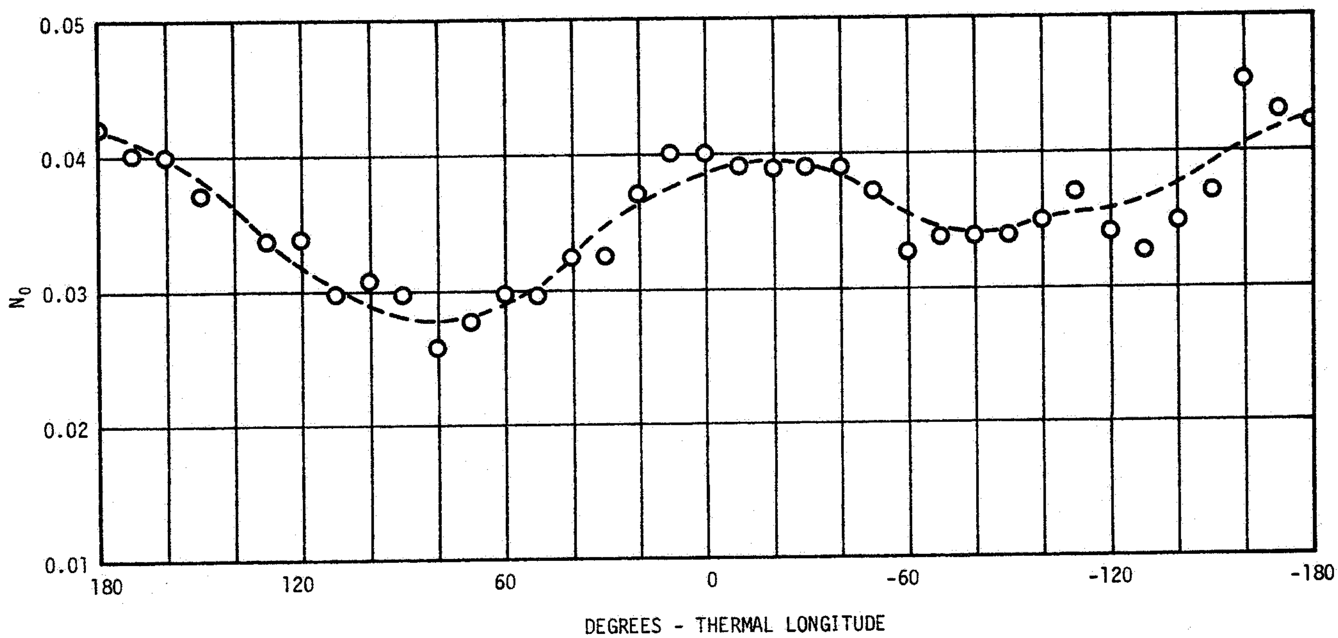

FIGURE 9. LOCAL N_0 VALUES ALONG THE 30° THERMAL LATITUDE

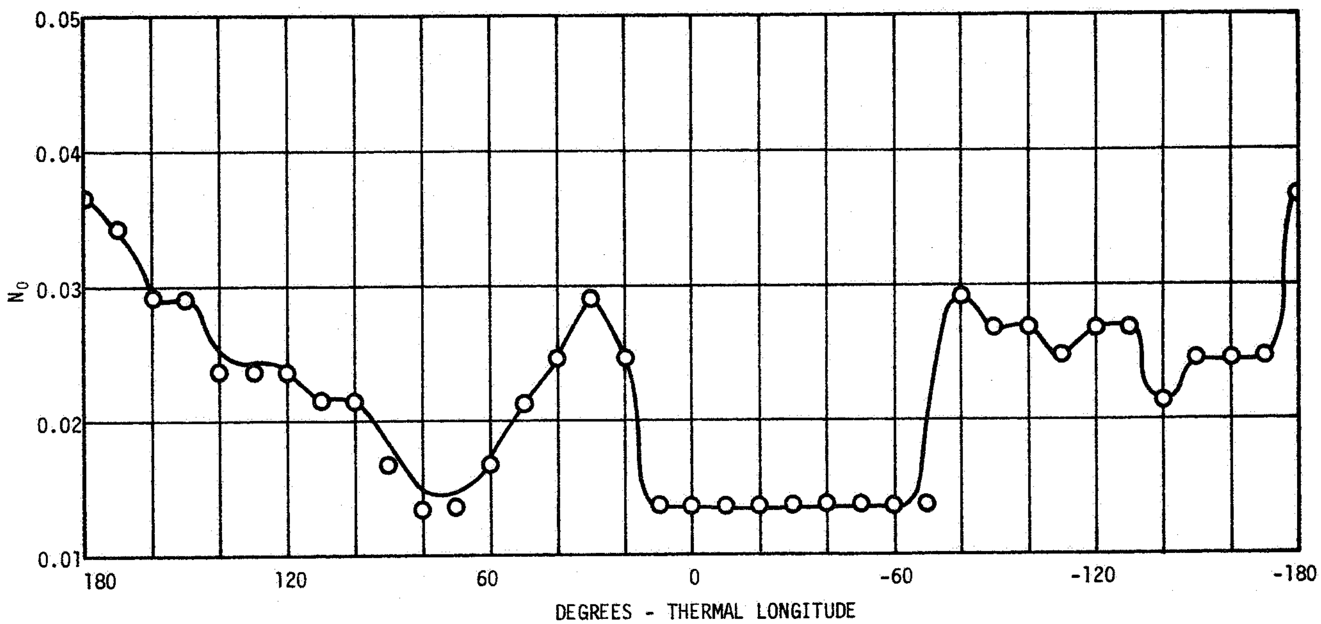

FIGURE 10. LOCAL N_0 VALUES ALONG THE 40° THERMAL LATITUDE

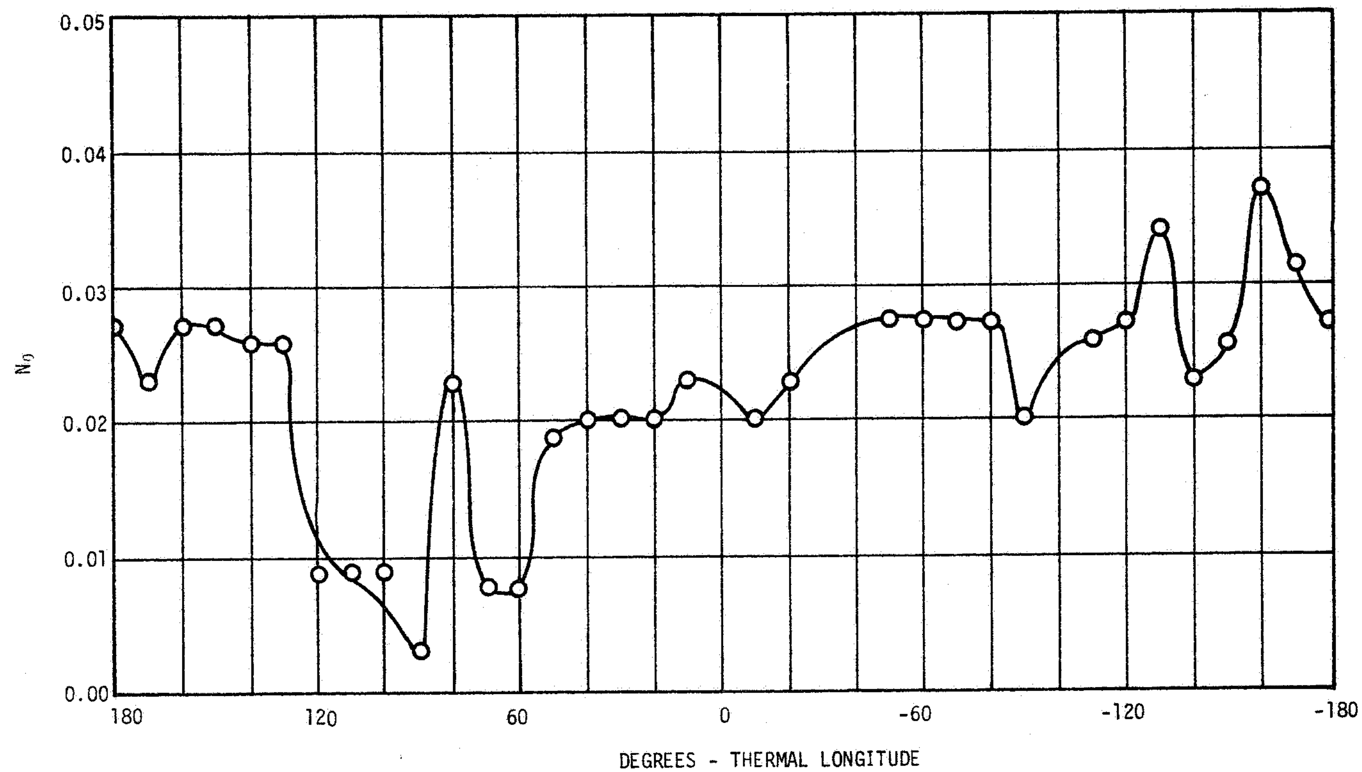

FIGURE 11. LOCAL N_0 VALUES ALONG THE 50° THERMAL LATITUDE

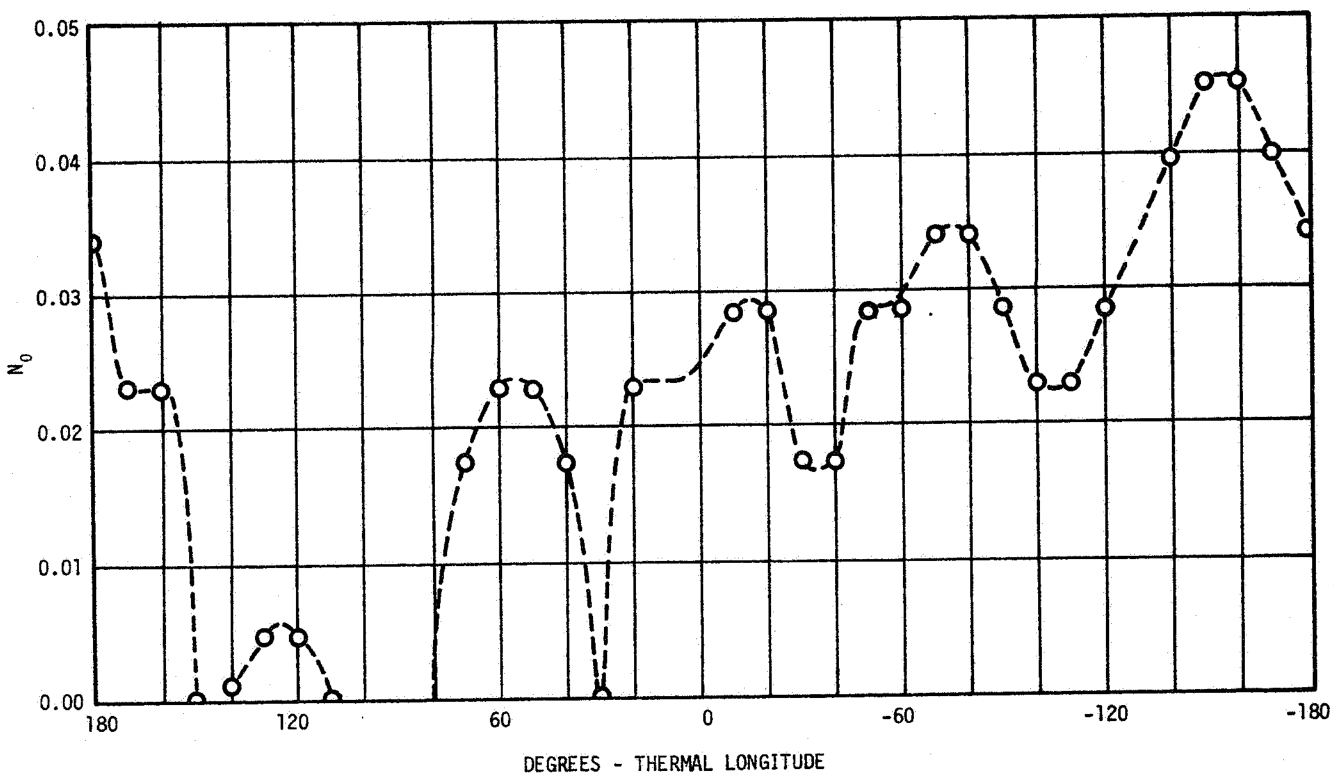

FIGURE 12. LOCAL N_0 VALUES ALONG THE 60° THERMAL LATITUDE

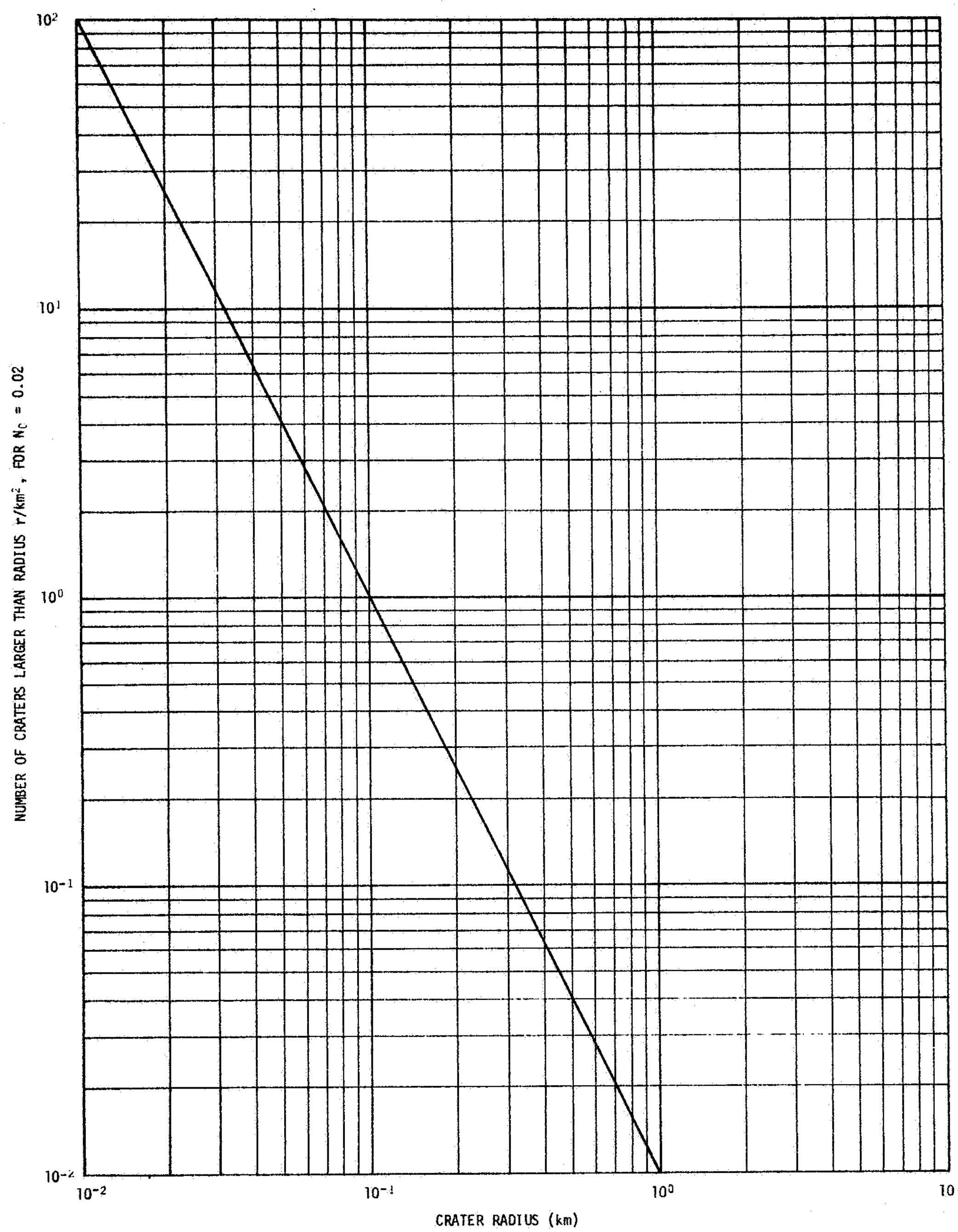

FIGURE 13. CUMULATIVE LOCAL LUNAR CRATER DISTRIBUTION FOR N_0 = 0.02
[PLOT OF $N' = (1/2)\ N_0\ r^{-2}$]

REMARKS AND CONCLUSIONS

It has been shown that this theory explains the qualitative characteristics of the thermal radiation observations. This model of hemispherical craters predicts that the limbs of the full moon disk radiate a higher intensity than is expected for a smooth Lambert sphere. The fairly close agreement between the calculated crater density and the measured density illustrates the validity of this geometric model.

The assumptions that have been made are all reasonable and can, with the exception of uniform temperature, be almost considered facts. The temperature of the sunlit portion of the crater is probably hotter than an equivalent flat area due to reradiation effects. This would tend to increase the subsolar point temperature in which case the temperature of the flat area would be less than that previously calculated from thermal radiation measurement. This view is also supported by Sinton (Ref. 8) who comments "valleys will be hotter than the peaks".

The calculated values for the crater densities are possibly too large because of the assumptions and restrictions leading to the development of Equation 42. The actual craters vary in shape and are certainly not hemispherical. Craters of one meter and less only tend to make the surface diffuse when viewed with a resolution radius of 10 kilometers or more.

The density of craters calculated for specific points on the Moon's surface yields a lunar wide distribution pattern. It is not the main intent of this investigation to develop this crater distribution but is strictly a byproduct. Through this model, a crater distribution can be calculated for any selected lunar landing site by utilizing thermal radiation data from that exact location. The range of the crater size predicted in these calculations is of the size that would hamper and endanger a lunar exploration team.

REFERENCES

1. Pettit, E., and Nicholson, S. B. (1930) "Lunar Radiation and Temperatures" Astrophys. J. 71, 102-135

2. Markov, A. V. (1924) "Les Particularities dans la Reflexion de la Lumiere par la Surface de la Lune", Astron. Nachr. 221, 65-78

3. Schoenberg, E. (1925) "Untersuchung zur Theorie der Beleuchtung des Mondes" Acta Soc. Fenn. 50

4. McGillem, C. D. and Miller, B. P. (1962) "Lunar Surface Roughness from Crater Statistics" J. Geophys. Res 67, 4787-4794

5. Ingrao, H. C., Young, A. T., and Linsky, J. L. (1966) "A Critical Analysis of Lunar Temperature Measurements in the Infrared", In "The Nature of the Lunar Surface, Proceedings of the 1965 IAU-NASA Symposium (W. N. Hess, D. H. Menzel, and J. A. O'Keefe, ed.) The Johns Hopkins Press, Baltimore, Maryland

6. Montgomery, C. G., Saari, J. M., Shorthill, R. W., and Six, W. F., Jr., (1966) "Directional Characteristics of Lunar Thermal Emission" Brown Eng. TN R-213, Boeing Doc. D1-82-0568

7. Miller, B. P. (1965) "Distribution of Small Lunar Craters Based on Ranger 7 Photographs" J. Geophys. Res 70, 2265-2266

8. Sinton, W. M., (1962) "Temperatures on the Lunar Surface", In Physics and Astronomy of the Moon" (Z. Kopal, ed.) Academic Press, New York

BIBLIOGRAPHY

1. Baldwin, R. B. (1965) "The Crater Diameter - Depth Relationship from Ranger VII Photographs" Astron. J. 70, 545-547

2. Bennett, A. L. (1938) "A Photovisual Investigation of the Brightness of 59 Areas on the Moon" Astrophys. J. 88, 1-26

3. Brinkman, R. T. (1966) "Lunar Crater Distribution from the Ranger VII Photographs" J. Geophys. Res 71, 340-342

4. Marcus, A. H. (1964) "A Stochastic Model of the Formation and Survival of Lunar Craters I. Distribution of Diameter of Clean Craters. Icarus 3, 460-472

5. Marcus, A. H. (1966a) "A Stochastic Model of the Formation and Survival of Lunar Craters II. Approximate Diameter Distribution of all Observable Craters. Icarus 5, 165-177

6. Marcus, A. H. (1966b) "A Stochastic Model of the Formation and Survival of Lunar Craters V. Approximate Diameter Distribution of Primary and Secondary Craters. Icarus 5, 590-605

7. Smith, Bruce G. (1967) "Lunar Surface Roughness--Shadowing and Thermal Emission" J. Geophy. Res. 72, 4059-4067

DOCUMENT CONTROL DATA - R&D

(Security classification of title, body of abstract and indexing annotation must be entered when the overall report is classified)

1. ORIGINATING ACTIVITY *(Corporate author)* Research Laboratories Brown Engineering, A Teledyne Company	2a. REPORT SECURITY CLASSIFICATION Unclassified 2b. GROUP N/A

3. REPORT TITLE

Crater Effects on Full Moon Directionality of Lunar Thermal Radiation

4. DESCRIPTIVE NOTES *(Type of report and inclusive dates)*
Technical Note, December 1967

5. AUTHOR(S) *(Last name, first name, initial)*

Doty, J. P.

6. REPORT DATE	7a. TOTAL NO. OF PAGES	7b. NO. OF REFS
December 1967	32	8

8a. CONTRACT OR GRANT NO. NAS8-20166 b. PROJECT NO. None c. d.	9a. ORIGINATOR'S REPORT NUMBER(S) TN R-252 9b. OTHER REPORT NO(S) *(Any other numbers that may be assigned this report)* None

10. AVAILABILITY/LIMITATION NOTICES

None

11. SUPPLEMENTARY NOTES None	12. SPONSORING MILITARY ACTIVITY Space Sciences Laboratory George C. Marshall Space Flight Center

13. ABSTRACT

A geometrical model of the lunar surface has been used to explain the directionality of the lunar thermal radiation from the full moon. From the model and measured data, an estimate of the crater density in certain locales has been calculated. The model assumes a lunar surface with hemispherical craters. A perturbation on the radiation intensity, caused by these craters, is added to Lambert's radiation cosine law. The resulting equation agrees very well with experimental data. With the resulting equation and a general crater distribution of $N = N_0 \, r^{-3}$, the local crater density is calculated.

14. KEY WORDS

lunar radiation
lunar crater model
lunar thermal properties
non-Lambert surface